Hindawi Publishing Corporation
Advances in Materials Science and Engineering
Volume 2014, Article ID 498674, 8 pages
http://dx.doi.org/10.1155/2014/498674

Research Article

Tensile Testing with Cyclic Strain Holding to Analyze Dynamic Recrystallization of Pure Lead

Mayu Muramatsu,[1] Motomichi Koyama,[2] and Ikumu Watanabe[2]

[1] *Advanced Manufacturing Research Institute, National Institute of Advanced Industrial Science and Technology, 1-2-1 Namiki, Tsukuba, Ibaraki 305-8564, Japan*
[2] *Research Center for Strategic Materials, National Institute for Materials Science, 1-2-1 Sengen, Tsukuba, Ibaraki 305-0047, Japan*

Correspondence should be addressed to Ikumu Watanabe; watanabe.ikumu@nims.go.jp

Received 12 February 2014; Accepted 18 March 2014; Published 14 April 2014

Academic Editor: Peter Majewski

Copyright © 2014 Mayu Muramatsu et al. This is an open access article distributed under the Creative Commons Attribution License, which permits unrestricted use, distribution, and reproduction in any medium, provided the original work is properly cited.

We analyzed the dynamic recrystallization of pure lead by tensile testing with cyclic strain holding at room temperature. The specimens were held at an identical strain and subsequently reloaded, providing the strength before and after the strain holding process. The difference in strength enables factors affecting dynamic recrystallization behavior to be analyzed through mechanical testing. For instance, the effects of strain rate on dynamic recrystallization were analyzed by comparing the results obtained from tensile tests with and without strain holding. This experimental technique demonstrated some parts of contribution of elastic strain, dynamic recovery, dynamic recrystallization, and necking to stress-strain responses.

1. Introduction

Low yield stress and work hardening capacity of pure lead are important for its application in damping materials. Low yield stress is a prerequisite for damping materials because these materials should deform plastically before the plastic deformation of the main body when affected by an accidental force like that encountered in an earthquake. Further, low work hardening capacity is imperative for the continued use of dampers. Depending on the work hardening behavior, a plastic strain is introduced in the main body when the flow stress of the damper reaches the yield stress of the main body. In order to prevent this plastic deformation of the main body, the damper is required to show low work hardening capacity as well as low yield stress. The work hardening capacity of pure lead is sufficiently low, particularly at low strain rates, because dynamic recrystallization (DRX) occurs even at room temperature due to the low melting temperature [1–3]. These facts enable pure lead to be used as a practical damping material. Therefore, the important factors to be considered for the application of pure lead as a damper are yield stress and work hardening capacity related to dislocation density evolution and the progress of DRX. In this work, we note the microstructure aspects associated with dislocation density and DRX.

The DRX behavior and dislocation density evolution of pure lead can be analyzed by correlating the microstructural aspects through a theoretical approach. Bailey-Hirsch's equation [4] simply provides the relationship between dislocation density and flow stress. Numerous models on DRX also have been established conventionally [5–11]. The most renowned model was proposed by Luton and Sellars [12]. The stress-strain behavior was explained by critical strain ε_c and recrystallization strain ε_x, where ε_c and ε_x were defined as the strains at a peak stress and at recrystallization completion, respectively. Other studies attempted to explain this model on the basis of dislocation density, grain boundary energy, and diffusion velocity [13–15]. These models have been validated for steel [16–21], copper [22–24], nickel [25], aluminum [26], and various alloys [27–33]. However, there are only a few experimental reports on the deformation behavior relating to the DRX in pure lead [34–36]. This is because, due to the occurrence of recrystallization at room temperature in pure lead, microstructure observations to analyze the progress of DRX and to detect the change in the dislocation densities are significantly challenging. Thus, experimental analyses of

DRX in pure lead need unique method containing factors affecting the progress of recrystallization and the dislocation density evolution.

In this paper, we provide and discuss some experimental results obtained by cyclic strain holding tests to analyze DRX in pure lead. In these tensile tests, strain holding was conducted at constant temperature, that is, room temperature. The degree of progress in recrystallization depends on experimental duration, strain, strain rate, and test temperature [1, 37]. Here, note that static recrystallization (SRX) occurred during strain holding. The difference between DRX and SRX is whether a specimen is under deformation or not when showing recrystallization [1, 2]. The dominant factors affecting SRX and DRX are the same, that is, stored dislocation energy, temperature, and experimental duration. Here, the magnitude of softening by DRX was assumed to be equal to that by SRX in terms of dislocation density. Therefore, the contribution of DRX to stress-strain responses is approximated by the combination of hardening by deformation and softening due to recrystallization at the same test temperature. Strain holding could regulate the experimental duration at a specific strain, implying that the tests can demonstrate various stress-strain responses with different magnitudes of progress in recrystallization. Hence, the comparative study of the results obtained from tests with and without strain holding can provide vital information that can assist in correlating the aforementioned factors with the stress-strain responses of pure lead. In this paper, we attempt to interpret the experimental results to gain an understanding of the DRX behavior of pure lead.

2. Experimental

Tensile specimens ware cut from 4.0 mm thick pure lead sheets (with the chemical composition as shown in Table 1) by spark machining. The specimens were subsequently solution treated at 400 K for 3.6 ks under air. Figure 1 is the rolling direction-inverse pole figure (RD-IPF) which was taken in the as-solution-treated condition. The experimental condition of this electron backscatter diffraction (EBSD) analysis will be shown later. Tensile tests were conducted at the ambient temperature (i.e., 298 K, which is half the melting point of pure lead) at various strain rates. The strain rates were varied from 1.7×10^{-5} to $1.7 \times 10^{-2}\,s^{-1}$. The gage dimension of each of the tensile specimens used in the present study was fixed at 4.0 mm (width) × 4.0 mm (thickness) × 30 mm (length). The specimens consisted of grip sections on both ends, which were fixed in an Instron-type machine. The strains were determined by dividing the displacements by the initial gage length.

The tensile tests with strain holding were also conducted at ambient temperature. Figure 2 shows the flow chart indicating the various steps of the cyclic strain holding tests. Initially, the specimen was deformed to 3.3% plastic strain (operation A), following which the specimen was held at this strain for 1,800 or 10,800 s (operation B). After the completion of one cycle, the straining was repeated; that is, the specimen was deformed again at the same strain rate to achieve

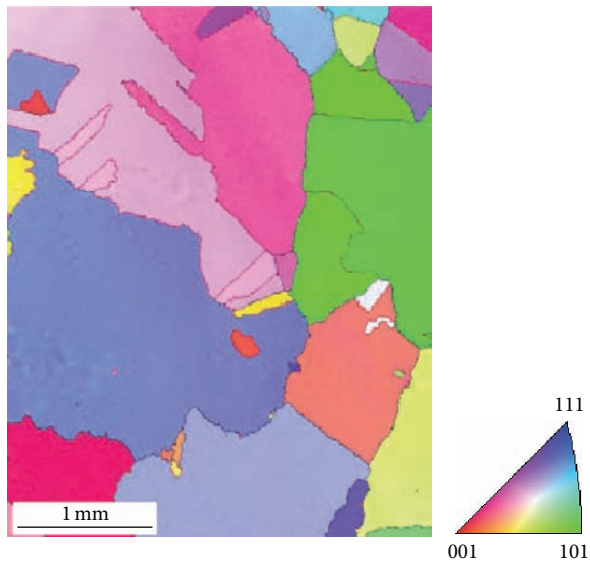

Figure 1: RD-IPF map in the as-solution-treated condition.

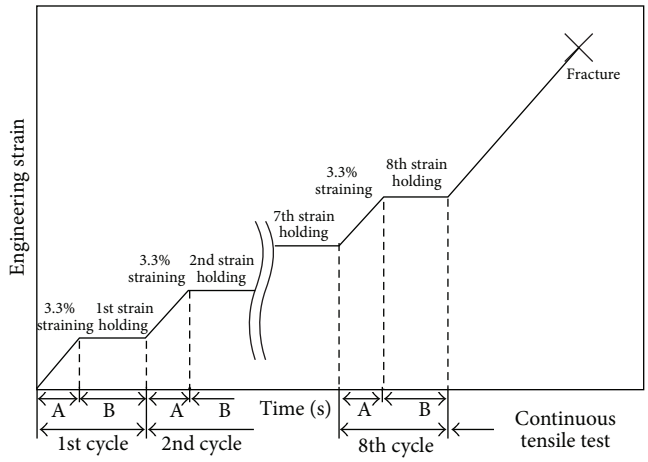

Figure 2: Schematics representing the experimental procedure used in the strain holding tests.

the initial deformation. After the completion of eight cycles, we conducted continuous tensile testing, in which the specimen was deformed to fracture at the same strain rate as that used to obtain the initial deformation.

Figure 3 is a schematic illustrating the significant of what the cyclic strain holding tests demonstrates. During the initial straining process (operation A), the stress increased with strain due to work hardening until the flow stress σ_{flow1} was reached after 0.2% proof stress $\sigma_{0.2}$. Then, during the strain holding step (operation B), stress decreased gradually to σ_{min2} due to relaxation and dynamic recrystallization. During the subsequent straining operation, stress took the values of σ_{reload} and σ_{flow}. The difference between $\sigma_{0.2}$ and $\sigma_{reload2}$ corresponded to the change in the dislocation density originating from straining. The difference between σ_{flow1} and $\sigma_{reload2}$ corresponded to the decrease in dislocation density arising because of recrystallization during the last strain

Table 1: Chemical composition of the lead specimen used in the present study.

	Pb	Sb	Cu	Sn	Fe	Bi	Zn	Ag	As
Component (wt.%)	99.99	<0.002	<0.0005	<0.002	<0.0005	<0.002	<0.0005	<0.0005	<0.002

Table 2: Experimental conditions in the present study.

Index	Strain rate (s^{-1})	Duration of strain holding (s)	Unloading
1	1.7×10^{-2}	×	×
2		300	○
3		300	×
4		1800	×
5		10800	×
6	1.7×10^{-3}	×	×
7	1.7×10^{-4}	×	×
8	1.7×10^{-5}	×	×
9		1800	×

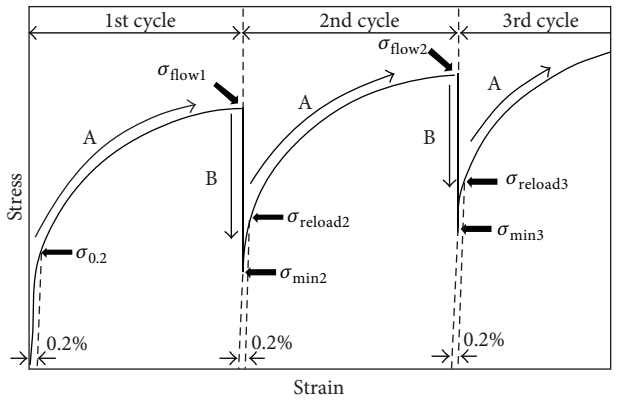

Figure 3: Schematics representing the stress-strain responses occurring during the strain holding process.

holding step. In addition, the change in stress from σ_{min2} to $\sigma_{reload2}$ was caused by relaxation. To investigate DRX, we performed several experiments with and without strain holding whose conditions are shown in Table 2.

In the microstructural observations using EBSD analysis, the specimens were chemically polished with mixed aqueous solution, 20% hydrogen peroxide and 80% acetic acid, at 298 K after mechanical polishing. The EBSD analyses were conducted at 294 K at 20 kV. A tensile-deformed specimen used for the EBSD analysis was immersed into liquid nitrogen immediately after the tensile test to suppress SRX at room temperature.

3. Results and Discussion

3.1. Tensile Properties Associated with DRX. Figure 4 shows the engineering stress-strain curves obtained at various strain rates (Indices 1, 6, 7, and 8 in Table 2). The work hardening was suppressed with decreasing strain rate, which led to

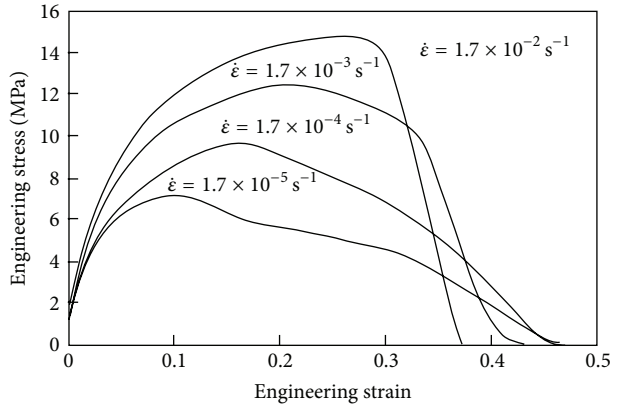

Figure 4: Engineering stress-strain curves obtained at various strain rates.

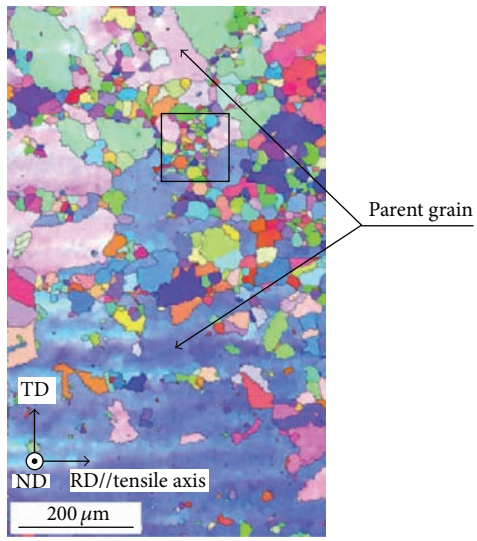

Figure 5: RD-IPF map after fracture at strain rate of $\dot{\varepsilon} = 1.7 \times 10^{-5}\ s^{-1}$.

decreases in the ultimate tensile strength (UTS) and uniform elongation. A microstructure observation was conducted by using EBSD to interpret the reduction in work hardening rate, UTS, and uniform elongation. Figure 5 is a RD-IPF map taken from the specimen fractured at the strain rate of $1.7 \times 10^{-5}\ s^{-1}$. The observed part was selected from uniformly deformed gauge part. The parent grain is indicated by the black arrow. (Parent grains are determined by the grains that existed in the solution-treated condition.) Lots of small grains with the size of 10–20 μm were observed near the boundaries of the parent grain as indicated by the square. These small grains have newly generated near the grain boundaries by SRX or DRX since the sizes of

the small grains are much smaller than the ones of the parent grains as well as of the as-solution-treated condition. Grain boundaries are supposed to be strain concentration sites [38], which preferentially initiated the recrystallization around the parent grain boundaries. This fact observed in the uniformly deformed part indicates that the strain provided by the tensile test achieved the critical strain for recrystallization before reaching UTS. Therefore, the suppression of work hardening with the decrease in strain rate is attributed to dynamic recovery as well as DRX, as conventionally reported [1]. The decrease in strain rate provides a longer duration per strain, promoting the recovery and recrystallization. The decreases in uniform elongation and UTS are also caused by the decreasing work hardening rate, which is clarified through Considère's Criterion. However, the simple tensile test cannot clarify each contribution from phenomena to the decrease in flow stress: dynamic recovery, DRX, and necking. Tensile tests with strain holding tests are expected to clarify some parts of the contribution, which is demonstrated from the next section.

3.2. Testing with and without Unloading. To clarify the contribution of dynamic recovery and recrystallization to the deformation behavior, factors affecting the stress-strain response need to be investigated. We here note that an influence of elastic strain on dynamic recovery and DRX. The dynamic recovery and recrystallization are driven by stored energy during the deformation, which can be separated into elastic and plastic energies. Figure 6 is a schematic representation of the elastic and plastic portions of stress-strain curve during the strain holding test accompanied by unloading. Figure 7 shows the results of the cyclic strain holding tests carried out with and without unloading (Indices 2 and 3 in Table 2), which are depicted by broken and solid lines, respectively. The elastic energy can be calculated by the stress during the strain holding test with unloading (as shown in Figure 6). The difference between the stresses in the two tests corresponds to the contributions of the elastic strain energy to recovery and recrystallization during strain holding. As can be seen, the stress-strain responses with unloading showed almost similar values as the ones obtained without unloading, indicating that the effect of elastic strain energy on the recrystallization of pure lead was negligible. Thus, we considered only the effect of plastic strain in this study.

3.3. Testing with and without Strain Holding. The stress-strain behaviors with and without strain holding are mentioned in this section. Figure 8 exhibits a comparative study of the results obtained from the tests carried out with and without strain holding. The broken and solid lines are engineering stress-strain curves obtained at the strain rate of 1.7×10^{-5} s^{-1} with and without strain holding for 1,800 s, respectively (Indices 8 and 9 in Table 2). The dotted lines connect $\sigma_{0.2}$ and each σ_{reload}. There were no significant differences between the flow stresses in the tests with and without strain holding until the third cycle. During the fourth cycle, both flow stresses began to decrease abruptly, and subsequently,

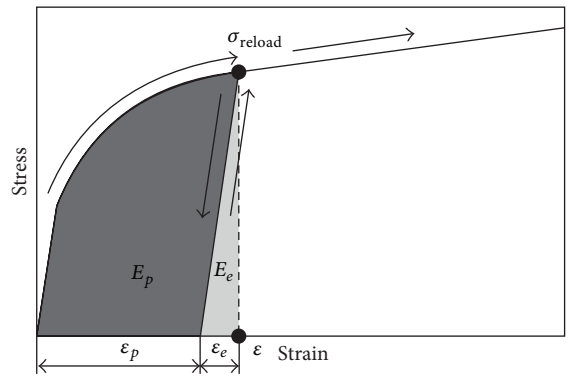

Figure 6: Schematic representation of the elastic and plastic region in stress-strain curves obtained from the strain holding tests carried out with unloading.

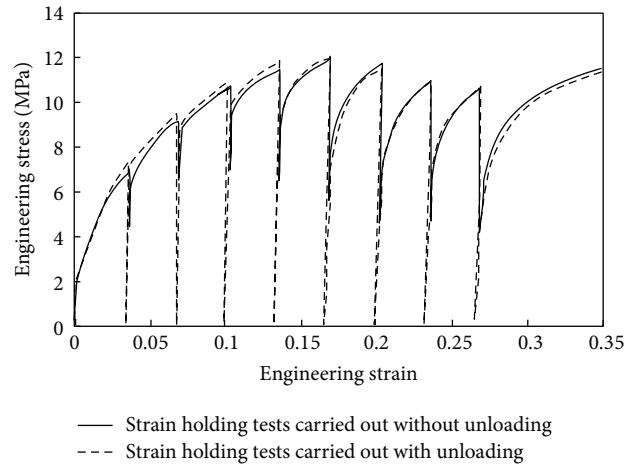

Figure 7: Engineering stress-strain curves obtained from strain holding tests carried out with and without unloading.

the flow stresses decreased further with increasing number of cycles. These results indicate the following points about DRX of pure lead during straining at the rate of 1.7×10^{-5} s^{-1}.

(A) The strain provided during the first three cycles reached a critical value to trigger recrystallization [12]. The stress drop that occurred after the attainment of the UTS was initially caused by the occurrence of DRX [1].

(B) Accordingly, the dependence of flow stress on strain rate before the specimens were strained to 10% can be thought to arise from dynamic recovery, since the recrystallization cannot occur before 10% which corresponds to the cumulative strain till the third cycle.

Although the degree of progress of recrystallization occurring during the experiments with strain holding was anticipated to be more significant than that occurring during continuous deformation, after the third cycle, the flow stresses observed in the strain holding test were higher than those encountered during continuous deformation partially.

This is considered to be caused by necking. As long as flow stress decreases, as shown in the stress-strain response of the continuous deformation experiments, occurrence of necking becomes significant with increasing plastic strain. In contrast, the work hardening capacity observed during the strain holding experiment was recovered in each strain holding cycle because of the SRX. Such recovery brought about significant work hardening during subsequent straining, which suppressed the necking and led to the higher flow stresses than those in continuous tensile deformation.

As can be seen from the results of the continuous tensile testing experiments, the tendency of stress decrease can be separated into three parts. Initially, (i) a sharp decrease occurred, which was followed by (ii) a marginal decrease, and subsequently, (iii) a sharp decrease was observed once again. Considering the stress changes accompanying necking, the first sharp decrease can be attributed to the combined effect of dynamic recrystallization and necking. The marginal decrease was caused dominantly by necking, because DRX was considered to have been completed already. The change in the slope of the stress decrease can be anticipated to correspond to the conventionally reported serrations arising from the alternating achievement of critical and recrystallization strains that are defined as the critical strain required for DRX and the strain at which recrystallization is complete [12]. Although it is difficult to interpret, the critical strain and recrystallization strain can be found in the results of the continuous tensile test.

The stress-strain response obtained by strain holding test represented the sharp decrease beginning at the third cycle. The difference between σ_{flow} and σ_{min}, that is, σ_{flow3} and σ_{min4}, became abruptly significant, because the strain reached the critical strain. Subsequently, a marginal decrease in stress was observed at the fourth strain holding step. The magnitude of the difference between σ_{flow4} and σ_{min5} was smaller than that between σ_{flow3} and σ_{min4}. This strain was considered to be the recrystallization strain [12]. The second sharp decrease occurred when the critical strain required for DRX was reached again. Accordingly, a relatively large difference between σ_{flow} and σ_{min} during the strain holding experiments can be expected to show the attaining the critical strain.

Additionally, the duration of straining in one cycle is almost identical to that for holding, and hence the dotted lines can be assumed to represent the stress-strain curve at a lower strain rate. Hereafter, such dotted curves connecting $\sigma_{0.2}$ and each σ_{reload} will be termed as virtual stress-strain curves in this paper. The assumption is confirmed by the features of these stress-strain curves such as suppressed work hardening and early achievement of UTS shown in Figure 4. The validity of this discussion will be reconsidered with virtual stress-strain curves in Figures 9 and 10.

3.4. Tests with Strain Holdings at Different Strain Rates. The broken line in Figure 8 is the engineering stress-strain curve obtained at the strain rate of $1.7 \times 10^{-5}\,\text{s}^{-1}$ with strain holding for 1,800 s (Index 9 in Table 2). The solid lines in Figure 9 show the result of the cyclic strain holding test

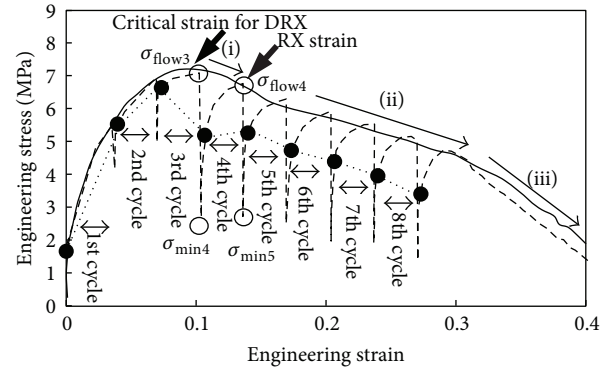

Figure 8: Engineering stress-strain curves obtained by tensile test with and without strain holding for 1,800 s at $\dot{\varepsilon}$ (strain rate) = $1.7 \times 10^{-5}\,\text{s}^{-1}$.

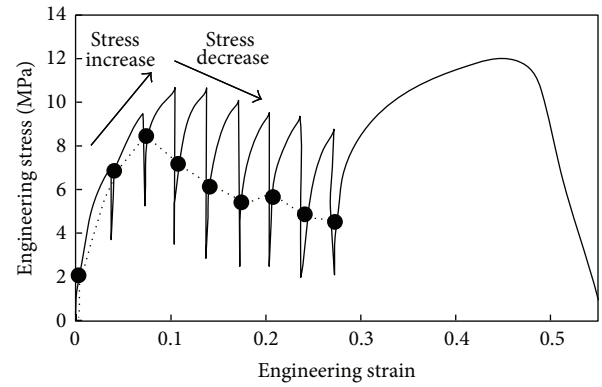

Figure 9: Engineering stress-strain curves obtained by tensile testing carried out with strain holding for 1,800 s at $\dot{\varepsilon} = 1.7 \times 10^{-2}\,\text{s}^{-1}$.

at the strain rate of $1.7 \times 10^{-2}\,\text{s}^{-1}$ with the strain holding for 1,800 s (Index 4 in Table 2). The difference between the experimental conditions in Figures 8 and 9 was the strain rate. Strain rates affect the flow stress, recrystallization, and dislocation density as discussed in Figure 4 in Section 3.1. It is particularly noted that the high σ_{flow} was observed at the high strain rate. The significant stress drops occurred in Figure 9 and the magnitude of stress drop decreased when the strain rate decreased as shown in Figure 8. The magnitude of stress drop indicates the degree of progress in SRX. At the same duration of strain holding, the degree of progress in SRX depends on the initial dislocation density that corresponds to the preceding flow stress σ_{flow} in terms of Bailey-Hirsch equation [39, 40]. The high σ_{flow} s at the strain rate of $1.7 \times 10^{-2}\,\text{s}^{-1}$ in Figure 9 means that DRX did not occur sufficiently at the short duration of straining, which results in the high dislocation density promoting SRX during the following strain holding.

3.5. Tests with Different Durations of Strain Holdings. In this section, we compare the results of tests with different durations of strain holdings to study the time dependency in recrystallization. As mentioned in the previous section, the solid lines in Figure 9 show the result of the cyclic strain

holding test at the strain rate of $1.7 \times 10^{-2}\ s^{-1}$ with the strain holding for 1,800 s (Index 4 in Table 2). The solid lines in Figure 10 show the result of cyclic strain holding test carried out at the strain rate of $1.7 \times 10^{-2}\ s^{-1}$ with the strain holding for 10,800 s (Index 5 in Table 2). The σ_{flow} s in Figure 10 took similar values after the second cycle. The recrystallization was almost complete during strain holdings for 10,800 s, which resulted in the almost constant σ_{flow}. Such similarity among σ_{flow} s was not seen in the first cycle and in the subsequent cycles in Figure 9, indicating that the recrystallization was almost complete during strain holding for 10,800 s though the recrystallization was not complete during strain holding for 1,800 s.

The dotted lines in Figures 9 and 10 were virtual stress-strain curves. The duration of straining per one cycle was less than 2 s at the strain rate of $1.7 \times 10^{-2}\ s^{-1}$ and was negligible when compared to the holding time of 1,800 and 10,800 s.

The experimental duration of Figure 9 was close to that of one of the continuous tensile tests carried out at the strain rate of $1.7 \times 10^{-5}\ s^{-1}$. As can be seen in Figure 4, the virtual stress-strain curve is similar to that obtained by continuous deformation at the strain rate of $1.7 \times 10^{-5}\ s^{-1}$ rather than that obtained at the strain rate of $1.7 \times 10^{-2}\ s^{-1}$ in terms of the tendencies of the work hardening and the value of UTS. However, in Figure 9, the specimen showed significant work hardening and uniform elongation after eight strain holding cycles, indicating that the deformation that occurred during the eight cycles was homogeneous. The virtual stress-strain curve obtained by cyclic strain holding tests at the strain rate of $1.7 \times 10^{-2}\ s^{-1}$ provides the advantage that the influence of necking in the continuous tensile tests (discussed in Section 3.3) can be eliminated. It is worth noting that σ_{reload} included the stress decrease arising from SRX occurring during strain holding. Instead of the change in slope shown in Figure 8, the stress increased and then decreased again in Figure 9, because the effect of necking was removed showing only the effect of SRX during the strain holdings in the virtual stress-strain curve. The repetitive stress change corresponds to the conventionally reported serrations arising from DRX, suggesting that the change of slope in the local elongation shown in Figure 8 was caused by recrystallization as well as by necking.

As shown in Figure 10, the deformation during the eight strain holding cycles was also homogeneous, due to the significant work hardening that occurred after cyclic strain holding. The important differences between the virtual stress-strain curve in Figure 10 and that in Figure 9 are the smaller critical strain and the larger number of cycles of serrations. The reduction in critical strain indicates that the initiation of the DRX was dominantly controlled by the holding time.

The variation in duration showed the same tendency as that of the strain rate dependence of the stress-strain response associated with DRX. The clear serrations observed in the virtual stress-strain curves are a typical phenomenon that is often reported in torsion and compression tests [6, 12, 23, 24]. Although tensile testing is simple, sometimes the occurrence of serration is difficult due to necking. In the tensile tests on pure lead carried out with cyclic strain holding at relatively high strain rates such as $1.7 \times 10^{-2}\ s^{-1}$, the influence of necking can be removed, which provides the existence of critical and recrystallization strains. In particular, clear serrations appearing in virtual stress-strain curves help to clarify DRX.

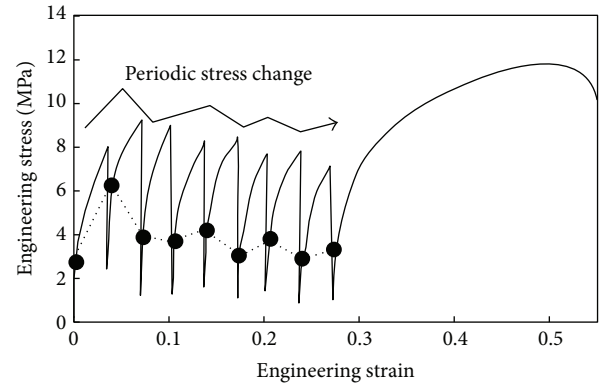

Figure 10: Engineering stress-strain curves obtained by tensile testing carried out with strain holding for 10,800 s at $\dot{\varepsilon} = 1.7 \times 10^{-2}\ s^{-1}$.

4. Conclusions

Dynamic recrystallization behavior in pure lead at room temperature was examined through tensile testing with strain holding. Comparative analyses between the tensile tests were carried out with and without cyclic strain holding characterized DRX in the usual continuous stress-strain response. The cyclic strain holding tests were demonstrated to be capable of clarifying the contribution of elucidating elastic strain, dynamic recovery, DRX, and necking to the tensile stress-strain response at various strain rates. Additionally, the stress change caused due to DRX in the continuous tensile tests was also clearly observed in virtual stress-strain curves obtained from the cyclic strain holding tests. From the virtual stress-strain curves, the critical and recrystallization strains were obtained. Further investigations involving simulations of the stress-strain responses of the experiments reported here are expected to reveal the details of the deformation behavior of pure lead at room temperature. Nevertheless, the cyclic strain holding method presented in this paper is a simple and helpful tool to analyze DRX.

Conflict of Interests

The authors declare that there is no conflict of interests regarding the publication of this paper.

Acknowledgments

The authors would like to express their thanks to Dr. Y. Kimura for permitting access to the tensile test machine, Dr. S. Ii for helping with the technics of the electrochemical polishing, and Mr. H. Yoshida for processing the lead specimens.

References

[1] F. J. Humphreys and M. Hatherly, *Recrystallization and Related Annealing Phenomena*, Elsevier, Oxford, UK, 2004.

[2] G. Gottstein, *Physical Foundations of Materials Science*, Springer, Berlin, Germanny, 2004.

[3] E. G. Thomsen, C. T. Yang, and S. Kobayashi, *Mechanics of Plastic Deformation in Metal Processing*, von Holtzbrinck Publishing Group, London, UK, 1965.

[4] D. J. Bailey and W. F. Flanagan, "The relationship between dislocation density and flow stress in materials deforming by a peierls-nabarro mechanism," *Philosophical Magazine*, vol. 15, no. 133, pp. 43–49, 1967.

[5] C. M. Sellars and W. J. McTegart, "On the mechanism of hot deformation," *Acta Metallurgica*, vol. 14, no. 9, pp. 1136–1138, 1966.

[6] J. J. Jonas, C. M. Sellars, and W. J. McG. Tegart, "Strength and structure under hot-working conditions," *International Materials Reviews*, vol. 14, no. 1, pp. 1–24, 1969.

[7] A. Najafizadeh, J. J. Jonas, G. R. Stewart, and E. I. Poliak, "The strain dependence of postdynamic recrystallization in 304 H stainless steel," *Metallurgical and Materials Transactions A: physical Metallurgy and Materials Science*, vol. 37, no. 6, pp. 1899–1906, 2006.

[8] N. D. Ryan and H. J. McQueen, "Dynamic softening mechanisms in 304 austenitic stainless steel," *Canadian Metallurgical Quarterly*, vol. 29, no. 2, pp. 147–162, 1990.

[9] E. I. Poliak and J. J. Jonas, "A one-parameter approach to determining the critical conditions for the initiation of dynamic recrystallization," *Acta Materialia*, vol. 44, no. 1, pp. 127–136, 1996.

[10] A. Laasraoui and J. J. Jonas, "Prediction of steel flow stresses at high temperatures and strain rates," *Metallurgical Transactions A*, vol. 22, no. 7, pp. 1545–1558, 1991.

[11] T. Sakai, Y. Nagao, M. Ohashi, and J. J. Jonas, "Flow stress and substructural change during transient dynamic recrystallization of nickel," *Materials Science and Technology*, vol. 2, no. 7, pp. 659–665, 1986.

[12] M. J. Luton and C. M. Sellars, "Dynamic recrystallization in nickel and nickel-iron alloys during high temperature deformation," *Acta Metallurgica*, vol. 17, no. 8, pp. 1033–1043, 1969.

[13] H. P. Stüwe and B. Ortner, "Recrystallization in hot working and creep," *Metal Science*, vol. 8, no. 6, pp. 161–167, 1974.

[14] R. Sandström and R. Lagneborg, "A model for hot working occurring by recrystallization," *Acta Metallurgica*, vol. 23, no. 3, pp. 387–398, 1975.

[15] W. Roberts, H. Boden, and B. Ahlblom, "Dynamic recrystallization kinetics," *Metal Science*, vol. 13, no. 3-4, pp. 195–205, 1979.

[16] A. Dehghan-Manshadi, M. R. Barnett, and P. D. Hodgson, "Recrystallization in AISI 304 austenitic stainless steel during and after hot deformation," *Materials Science and Engineering A*, vol. 485, no. 1-2, pp. 664–672, 2008.

[17] A. Dehghan-Manshadi, M. R. Barnett, and P. D. Hodgson, "Microstructural evolution during hot deformation of duplex stainless steel," *Materials Science and Technology*, vol. 23, no. 12, pp. 1478–1484, 2007.

[18] S.-I. Kim and Y.-C. Yoo, "Dynamic recrystallization behavior of AISI 304 stainless steel," *Materials Science and Engineering A*, vol. 311, no. 1-2, pp. 108–113, 2001.

[19] E. I. Poliak and J. J. Jonas, "Initiation of dynamic recrystallization in constant strain rate hot deformation," *ISIJ International*, vol. 43, no. 5, pp. 684–691, 2003.

[20] E. I. Poliak and J. J. Jonas, "Critical strain for dynamic recrystallization in variable strain rate hot deformation," *ISIJ International*, vol. 43, no. 5, pp. 692–700, 2003.

[21] T. Sakai, M. G. Akben, and J. J. Jonas, "Dynamic recrystallization during the transient deformation of a vanadium microalloyed steel," *Acta Metallurgica*, vol. 31, no. 4, pp. 631–641, 1983.

[22] W. Gao, A. Belyakov, H. Miura, and T. Sakai, "Dynamic recrystallization of copper polycrystals with different purities," *Materials Science and Engineering A*, vol. 265, no. 1-2, pp. 233–239, 1999.

[23] Y. V. R. K. Prasad and K. P. Rao, "Kinetics and dynamics of hot deformation of OFHC copper in extended temperature and strain rate ranges," *Zeitschrift fuer Metallkunde*, vol. 96, no. 1, pp. 71–77, 2005.

[24] Y. V. R. K. Prasad and K. P. Rao, "Kinetics of high-temperature deformation of polycrystalline OFHC copper and the role of dislocation core diffusion," *Philosophical Magazine*, vol. 84, no. 28, pp. 3039–3050, 2004.

[25] G. Gottstein and U. F. Kocks, "Dynamic recrystallization and dynamic recovery in <111> single crystals of nickel and copper," *Acta Metallurgica*, vol. 31, no. 1, pp. 175–188, 1983.

[26] A. L. Dons and E. Nes, "Nucleation of cube texture in aluminium," *Materials Science and Technology*, vol. 2, no. 1, pp. 8–18, 1986.

[27] A. Gholinia, I. Brough, J. Humphreys, D. McDonald, and P. Bate, "An investigation of dynamic recrystallisation on Cu-Sn bronze using 3D EBSD," *Materials Science and Technology*, vol. 26, no. 6, pp. 685–690, 2010.

[28] G. A. Osinkolu, M. Tacikowski, and A. Kobylanski, "Combined effect of AIN and sulphur on hot ductility of high purity iron-base alloys," *Materials Science and Technology*, vol. 1, no. 7, pp. 520–525, 1985.

[29] D. W. Livesey and C. M. Sellars, "Hot-deformation characteristics of Waspaloy," *Materials Science and Technology*, vol. 1, no. 2, pp. 136–144, 1985.

[30] M. Tacikowski, G. A. Osinkolu, and A. Kobylanski, "Segregation-induced intergranular brittleness of ultrahigh-purity Fe-S alloys," *Materials Science and Technology*, vol. 2, no. 2, pp. 154–158, 1985.

[31] F. J. Humphreys, P. B. Prangnell, and R. Priestner, "Fine-grained alloys by thermomechanical processing," *Current Opinion in Solid State and Materials Science*, vol. 5, no. 1, pp. 15–21, 2001.

[32] O. Covarrubias, O. Elizarrarás, and R. Colás, "Effect of heat treatment on mechanical properties of alloy 909," *Materials Science and Technology*, vol. 27, no. 6, pp. 1092–1097, 2011.

[33] O. Covarrubias, O. Elizarrarás, K. L. Kruger, and R. Colás, "Subscribed content heat treating of a ring rolled Ni-Fe-Cr superalloy," *Materials Science and Technology*, vol. 28, no. 2, pp. 192–196, 2012.

[34] I. Weiss, T. Sakai, and J. J. Jonas, "Effect of test method on transition from multiple to single peak dynamic recrystallization," *Metal science*, vol. 18, no. 2, pp. 77–84, 1984.

[35] S. Hotta, K. Matsumoto, T. Murakami, T. Narushima, and C. Ouchi, "Dynamic and static restoration behaviors of pure lead and tin in the ambient temperature range," *Materials Transactions*, vol. 48, no. 10, pp. 2665–2673, 2007.

[36] J. H. Nicholls and P. G. Mccormick, "Dynamic recrystallization in lead," *Metallurgical Transactions*, vol. 1, no. 12, pp. 3469–3470, 1970.

[37] M. Shaban and B. Eghbali, "Characterization of austenite dynamic recrystallization under different Z parameters in a

microalloyed steel," *Journal of Materials Science and Technology*, vol. 27, no. 4, pp. 359–363, 2011.

[38] C.-F. Yang, J.-H. Pan, and T.-H. Lee, "Work-softening and anneal-hardening behaviors in fine-grained Zn-Al alloys," *Journal of Alloys and Compounds*, vol. 468, no. 1-2, pp. 230–236, 2009.

[39] N. D. Ryan and H. J. McQueen, "Comparison of static softening in 300 series stainless steels under iso- and anisothermal conditions," *Materials Science and Technology*, vol. 7, no. 9, pp. 818–826, 1991.

[40] N. D. Ryan and H. J. McQueen, "Hot strength and microstructural evolution of 316 stainless steel during simulated multistage deformation by torsion," *Journal of Materials Processing Tech*, vol. 36, no. 2, pp. 103–123, 1993.

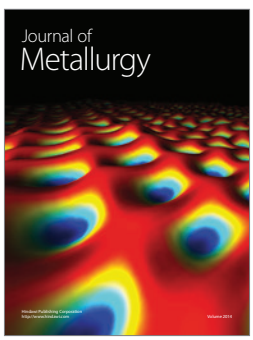

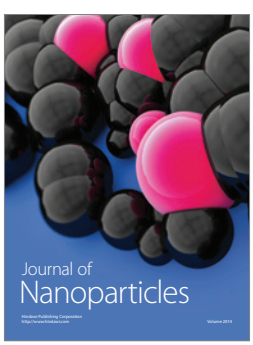

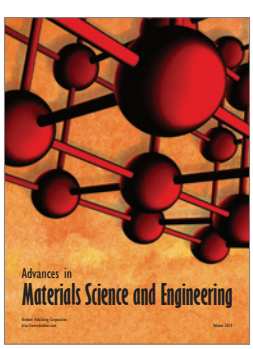

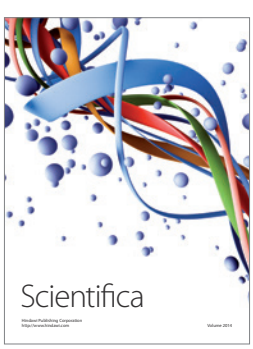

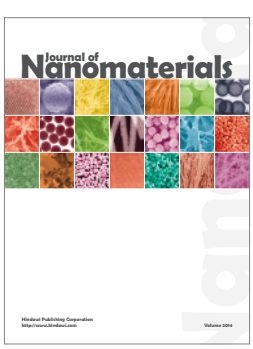

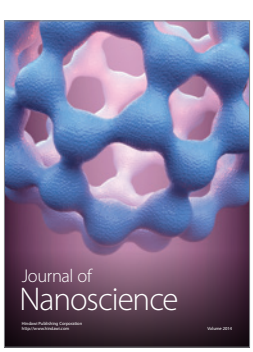

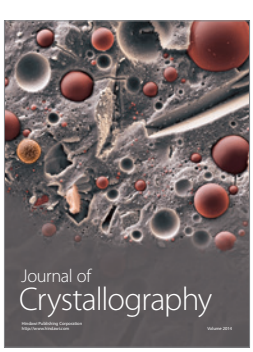

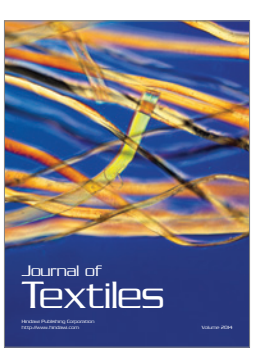

Hindawi

Submit your manuscripts at
http://www.hindawi.com